Journal of Alloys and Compounds 509 (2011) 2693–2696

Contents lists available at ScienceDirect

Journal of Alloys and Compounds

journal homepage: www.elsevier.com/locate/jallcom

Phase diagram of the quasi-binary system $TlInSe_2$–$SnSe_2$

M.Yu. Mozolyuk[a], L.V. Piskach[a], A.O. Fedorchuk[b], I.V. Kityk[c], I.D. Olekseyuk[a], O.V. Parasyuk[a,*]

[a] Department of Inorganic and Physical Chemistry, Lesya Ukraïnka Volyn National University, Voli Ave 13, 43025 Lutsk, Ukraine
[b] Department of Inorganic and Organic Chemistry, Lviv National University of Veterinary Medicine and Biotechnologies, Pekarska St., 50, 79010 Lviv, Ukraine
[c] Electrical Engineering Department, Czestochowa University of Technology, Al. Armii Krajowej 17/19, 42-200 Czestochowa, Poland

ARTICLE INFO

Article history:
Received 7 September 2010
Received in revised form
12 November 2010
Accepted 17 November 2010
Available online 23 November 2010

Keywords:
Quasi-binary system
Phase equilibria
X-ray powder diffraction
Solid solution

ABSTRACT

The $TlInSe_2$–$SnSe_2$ quasibinary system was investigated using differential thermal and X-ray phase analysis methods. The phase diagram is of eutectic type (V type of the Rozeboom classification). The solid solution range of the ternary compound in the $TlInSe_2$–$SnSe_2$ system extends to 28 mol.% $SnSe_2$ at 670 K. The eutectic point coordinates are 63 mol.% $SnSe_2$ and 788 K.

1. Introduction

An important place among the materials with interesting semiconductor properties belongs to the thallium-containing chalcogenides $TlC^{III}X_2$ and their analogs that form in the A^I–C^{III}–D^{IV}–X (A^I = Cu, Ag; C^{III} = Ga, In; D^{IV} = Ge, Sn; X = S, Se, Te) systems. For instance, $TlInSe_2$ is a ternary narrow-gap layered semiconductor; these are of interest due to a combination of high anisotropy, photoconductivity, segneto- and optoelectric, non-linear optical and magnetic properties suitable for versatile applications [1]. $SnSe_2$ belongs to a large class of $A^{IV}B^{VI}$ semiconductors which form a basis of modern IR optoelectronics and have found practical application in injection heterolasers, diodes and photosensors for mid- and far-IR ranges [2]. The investigation of the quasi-binary chalcogenide sections $A^IC^{III}X_2$–$D^{IV}X_2$ showed that the formation of the $A^IC^{III}D^{IV}X_4$ compounds is most common [3–11]. The crystal structures of these compounds follow interesting trends. The compounds also possess promising set of physical properties [12], this giving a push to the search of new materials with improved applied characteristics.

The literature lacks information on the phase diagram of the $TlInSe_2$–$SnSe_2$ system. Therefore the investigation of the component interaction at the $TlInSe_2$–$SnSe_2$ section was relevant. The investigation was also directed to the possible formation of a quaternary compound of the $TlC^{III}D^{IV}X_4$ type, an analog of respective silver- and copper-containing phases.

According to [2,13] $TlInSe_2$ and $SnSe_2$ melt congruently at 1053 K and 948 K, respectively. Thallium selenoindate crystallizes in S.G. *I*4/*mcm*, *a* = 0.8075 nm, *c* = 0.6847 nm [2]. Tin diselenide crystallizes in S.G. *P*-3*m*1, *a* = 0.3811 nm, *c* = 0.6137 nm [13].

2. Experimental procedure

A total of 12 samples were prepared for the investigation of the phase equilibria of the system. The batches were composed of high-purity metals and chalcogene: Tl 99.99 wt.%, In 99.99 wt.%, Sn 99.99 wt.%, and Se 99.999 wt.%. The compounds were synthesized by the single-temperature method in evacuated quartz containers in a shaft-type furnace. The maximum heating temperature was 1200 K, with 5 h exposure. The homogenizing annealing was held at 670 K for 250 h, followed by quenching the alloys into cold water. XRD reflection spectra were recorded by DRON 4-13 diffractometer with Ni-filtered CuK_α radiation (2θ range of 10–70°, with a step size of 0.05° and counting time of 2 s for the study of the phase equilibria; 2θ range of 10–100°, step size of 0.02°, and counting time of 10 s for the crystallographic refinement). The structure refinement was performed by full-profile Rietveld method using CSD software package [14]. Thermal analysis was performed using a Paulik–Paulik–Erdey derivatograph with a Pt/Pt–Rh thermocouple.

3. Results and discussion

Using the results of differential thermal analysis and XRD, the phase diagram of the quasi-binary system $TlInSe_2$–$SnSe_2$ was constructed. The diagram is of eutectic type (type V of the Rozeboom classification), with an invariant point at 63 mol.% $SnSe_2$ and 788 K (Fig. 1).

* Corresponding author. Tel.: +380 3322 49972; fax: +380 3322 41007.
E-mail address: oleg@univer.lutsk.ua (O.V. Parasyuk).

0925-8388/$ – see front matter © 2010 Elsevier B.V. All rights reserved.
doi:10.1016/j.jallcom.2010.11.112

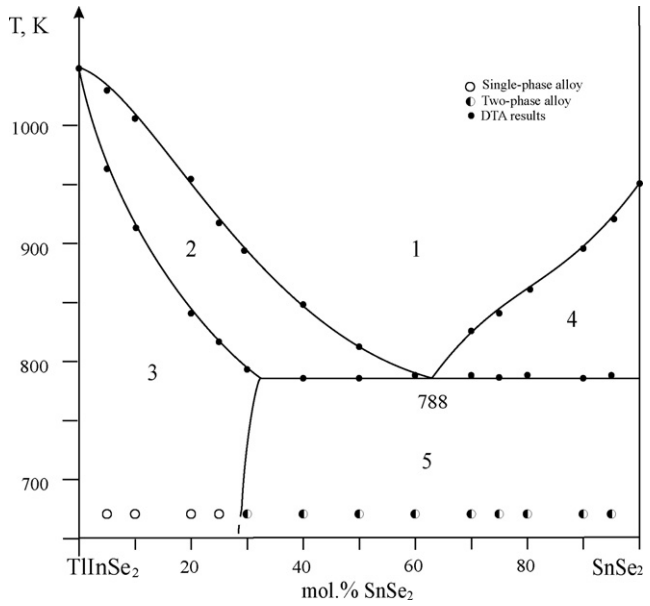

Fig. 1. Phase diagram of the $TlInSe_2$–$SnSe_2$ system. 1 – L; 2 – L + α; 3: α; 4 – L + $SnSe_2$; 5 – α + $SnSe_2$.

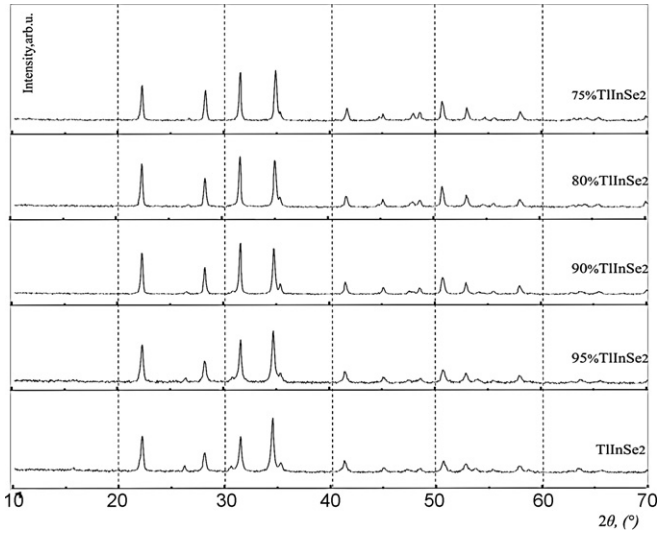

Fig. 2. Experimental diffraction patterns of the $TlInSe_2$–$SnSe_2$ section.

XRD investigation of the alloys of the $TlInSe_2$–$SnSe_2$ (in the range of 0–25 mol.% $SnSe_2$) indicates the absence of intermediate phases (Fig. 2). The diffraction pattern of the ternary compound agrees well with the literature data [15]. Further increase of the

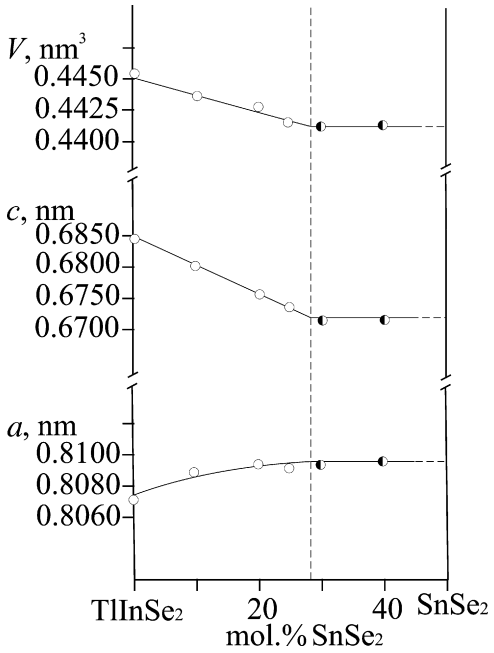

Fig. 3. Variation of unit cell parameters and volume of the alloys of the $TlInSe_2$–$SnSe_2$ system.

$SnSe_2$ content is accompanied by the converging of small reflections into the adjacent major peaks; this points out to the existence of a solid solution range of the ternary component of the studied section. According to the calculated lattice parameters, α-solid solution range extends from 72 to 100 mol.% $TlInSe_2$ at 670 K. The unit cell parameters of the alloys in this range are presented in Fig. 3.

The crystal structure of the solid solution alloy of 25 mol.% $TlInSe_2$ was investigated using the powder method. The conditions of the powder experiment and the crystallographic data for $Tl_{1-x}In_{1-x}Sn_xSe_2$ (x = 0–0.25) are summarized in Table 1.

The crystal structure of the $Tl_{1-x}In_{1-x}Sn_xSe_2$ (x = 0.25) was refined using the $NaInTe_2$ structure [16] as a model, with selenium atoms occupying the crystallographic site of Te, the statistical mix of In and Sn atoms occupying the site of In, and the Na site is occupied by 0.75 Tl + 0.25 vacancy. The atoms of the statistical mix possess a tetrahedral surrounding of Se atoms as shown in Fig. 4a, and Tl atoms have a tetragonal-antiprism surrounding of Se atoms (Fig. 4b).

The theoretical and experimental diffraction patterns of the $Tl_{1-x}In_{1-x}Sn_xSe_2$ (x = 0.25) are in good agreement (Fig. 5). The atomic coordinates and isotropic thermal parameters are listed for $Tl_{1-x}In_{1-x}Sn_xSe_2$ (x = 0–0.25) in Table 2.

Table 1
The results of the investigation of the $Tl_{1-x}In_{1-x}Sn_xSe_2$ (x = 0–0.25) crystal structure.

x	0	0.1	0.2	0.25
Space group			*I*4/*mcm* (No. 140)	
a, nm	0.80711(2)	0.80870(7)	0.80906(4)	0.80906(4)
c, nm	0.68372(1)	0.67997(7)	0.67604(1)	0.67438(4)
V, nm^3	0.4453(3)	0.447(1)	0.4430(2)	0.44143(7)
Radiation; wavelength, nm			Cu K_α; 0.154185	
Diffractometer			DRON 4-13	
Computation method			Full-profile	
Number of atom sites			3	
Number of free parameters			6	
Calculated density D_x, g/cm^3	7.116(4)	6.826(2)	6.552(2)	6.4242(9)
Absorption coefficient μm, 1/cm	1314.23	1247.88	1093.62	1130.68
2θ and $\sin\theta/\lambda_{(max)}$	99.59 and 0.495	99.46 and 0.495	99.59 and 0.495	99.55 and 0.495
Texture axis and parameter	[3 1 0] and 0.73(6)	[2 1 0] and 0.283(9)	[1 0 0] and 0.48(2)	[0 0 1] and 1.64(2)
R_I and R_P	0.0551 and 0.1124	0.0552 and 0.1116	0.0500 and 0.1267	0.0551 and 0.1044

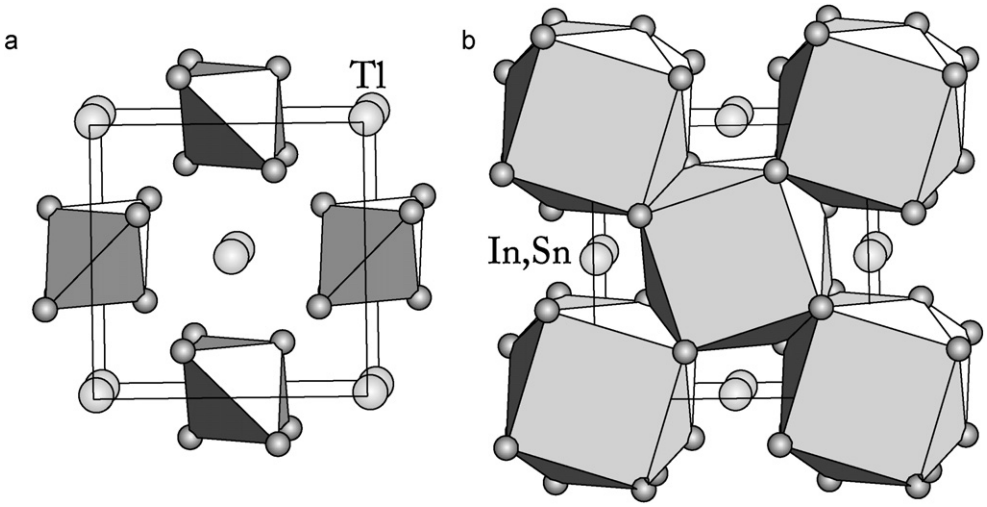

Fig. 4. Unit cell and coordination polyhedra of atoms in the structure of the $Tl_{1-x}In_{1-x}Sn_xSe_2$ solid solutions.

The solid solution range $Tl_{1-x}In_{1-x}Sn_xSe_2$ (x = 0–0.5) exhibits monotonely decreasing unit cell volume due to the subtraction of Tl atoms in the 4*a* site, that clearly cannot be compensated by the substitution of Sn atoms for In atoms. Uncommonly high values of thermal displacement parameters for Tl atoms can be explained by inter-atomic distances compared to the sum of respectively ionic radii ($r_{Tl^+} = 0.144$ nm) [17]. The Tl–Tl distances along the main axis are also somewhat elongated (d_{Tl-Tl} = 0.337 nm), which corroborate the high values of the Tl displacement parameters along this axis (Fig. 6). The tetragonal antiprism of Se atoms around Tl atoms also features somewhat elongated distances d_{Tl-Se} = 0.3438(2) nm.

Comparing the nature of the component interaction in the studied system with that in the systems $CuInSe_2$–$SnSe_2$ [8] and $AgInSe_2$–$SnSe_2$ [4], certain trends can be marked out. A^IInSnX_4 compounds (A^I = Cu, Ag; X = S, Se) that form in the copper- and silver-containing systems are characterized by incongruent melting. $CuInSnSe_4$ and $AgInSnSe_4$ crystallize in the tetragonal structure (S.G. $I\bar{4}$) with the lattice parameters a = 0.5670 nm, c = 1.134 nm and a = 0.5877 nm, c = 1.1284 nm, respectively. The investigated section $TlInSe_2$–$SnSe_2$ is of the eutectic type, with no formation of quaternary compounds. The extent of the homogeneity region of $TlInSe_2$ that reaches 28 mol.% $SnSe_2$ significantly exceeds that of the related above-mentioned systems, where the solid solubility does not exceed 5 mol.% for the copper-containing systems and 18 mol.% for the silver-containing systems. Considering the results of the investigation of the crystal structure of the boundary solid solution, we presume that the difference in the homogeneity regions of the ternary components is due to the size of the cations Cu^+, Ag^+ and

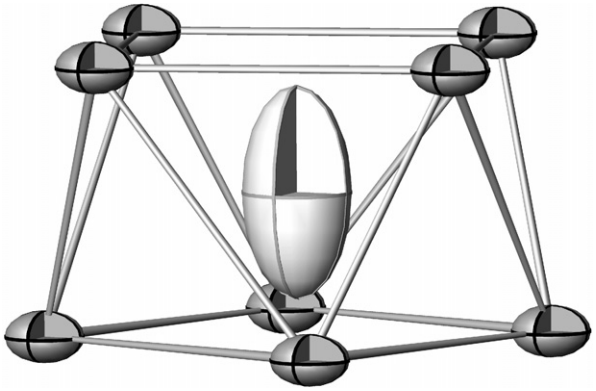

Fig. 6. Thermal displacement parameters of Tl (light ellipsoids) and Se (dark ellipsoids) atoms along the main axis for the $Tl_{1-x}In_{1-x}Sn_xSe_2$ (x = 0.25) alloy.

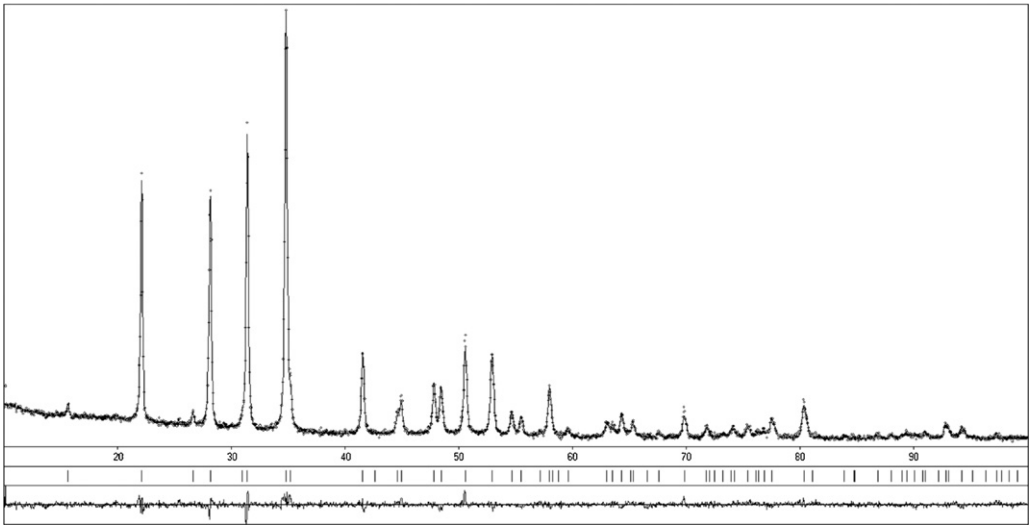

Fig. 5. Experimental, calculated and differential diffraction patterns of the solid solution alloy $Tl_{1-x}In_{1-x}Sn_xSe_2$ (x = 0.25).

Table 2
Atom coordinates and isotropic displacement parameters for $Tl_{1-x}In_{1-x}Sn_xSe_2$ ($x = 0$–0.25).

Atom	Wyckoff site	x	y	z	Site occupancy	$B_{iso} \times (10^2\,;\,nm^2)$
$Tl_{1-x}In_{1-x}Sn_xSe_2$ ($x = 0$)						
Tl	4*a*	0	1/2	1/4		1.68(9)
In	4*b*	0	0	1/4		1.14(13)
Se	8*h*	0.1721(9)	$x + 1/2$	0		0.85(14)
Interatomic distances						
In1–4Se1 0.2679(1) nm						
Tl1–4Se1 0.3421(1) nm						
$Tl_{1-x}In_{1-x}Sn_xSe_2$ ($x = 0.1$)						
Tl	4*a*	0	1/2	1/4	0.9Tl	4.14(8)
In	4*b*	0	0	1/4	0.9In + 0.1Sn	1.63(8)
Se	8*h*	0.1730(3)	$x + 1/2$	0		1.43(9)
Interatomic distances						
In1–4Se1 0.2608(2) nm						
Tl1–4Se1 0.3441(2) nm						
$Tl_{1-x}In_{1-x}Sn_xSe_2$ ($x = 0.2$)						
Tl	4*a*	0	1/2	1/4	0.8Tl	3.74(11)
In	4*b*	0	0	1/4	0.8In + 0.2Sn	1.47(9)
Se	8*h*	0.1727(3)	$x + 1/2$	0		1.01(9)
Interatomic distances						
In1–4Se1 0.2601(2) nm						
Tl1–4Se1 0.3439(2) nm						
$Tl_{1-x}In_{1-x}Sn_xSe_2$ ($x = 0.25$)						
Tl	4*a*	0	1/2	1/4	0.75Tl	3.77(6)
In	4*b*	0	0	1/4	0.75In + 0.25Sn	0.87(4)
Se	8*h*	0.1717(2)	$x + 1/2$	0		0.78(5)
Interatomic distances						
In1–4Se1 0.2589(1) nm						
Tl1–4Se1 0.3439(1) nm						

Tl^+. As a result, the tetrahedral coordination of atoms in the copper- and silver-containing compounds transforms into complex polyhedra (tetragonal antiprisms) with the coordination number 8 for the thallium-containing system.

References

[1] B.V. Lasarev, Z.Z. Kish, Y.Y. Peresh, Y.Y. Semrad, Complex Chalcogenides in the A^I–B^{III}–C^{VI} Systems, Metallurgy, Moscow, 1993 (in Russian).
[2] D.M. Bercha, Y.V. Voroshilov, V.Y. Slyvka, I.D. Turyanitsya, Complex Chalcogenides and Chalcogene-Halides, Leningrad, Vysshya Shkola, 1983 (in Russian).
[3] G.P. Gorgut, Ph.D. Thesis. Ivan Franko National University of Lviv, Lviv, 2002 (in Ukrainian).
[4] O.V. Krykhovets, Ph.D. Thesis. Ivan Franko National University of Lviv, Lviv, 1999 (in Ukrainian).
[5] O.M. Strok, O.F. Zmiy, I.D. Olekseyuk, Lviv Univ. Bull. 39 (2000) 72.
[6] G.G. Shabunina, T.G. Aminov, Zhurnal Neorg. Khim. 44 (1999) 859.
[7] A.P. Vakulovich, I.D. Olekseyuk, J. Alloys Compds. 367 (2004) 47.
[8] I.D. Olekseyuk, A.P. Vakulovich, O.V. Krykhovets, Proceedings of the VII Int'l Conference on Crystal Chemistry of Intermetallic Compounds, Lviv, Ukraine, 1999, p. pA15.
[9] H. Matsushita, A. Katsui, J. Phys. Chem. Sol. 66 (2005) 1933.
[10] O.V. Krykhovets, L.D. Gulay, I.D. Olekseyuk, J. Alloys Compds. 337 (2002) 182.
[11] T. Ohachi, B.R. Pamplin, Ternary Compounds, Inv. Contrib. Pap., 3rd Int'l. Conf., Edinburgh, 1977, p. 21.
[12] M.A. McGuire, T.J. Scheidemantel, J.V. Badding, F.J. DiSalvo, Chem. Mater. 17 (2005) 6186.
[13] N.K. Abrikosov, L.Y. Shelimova, AIVBVI-Based Semiconductor Materials, Nauka, Moscow, 1975 (in Russian).
[14] L.G. Akselrud, P.Y. Zavalij, Y.N. Grin', V.K. Pecharsky, B. Baumgartner, E. Wolfel, Mater. Sci. Forum 133 (1993) 335.
[15] D. Müller, G. Eulenberger, H. Hanh, Z. Anorg. Allg. Chem. 398 (1973) 207–220.
[16] E.R. Franke, H. Schaefer, Anorg. Chem. 27 (1972) 1308–1315.
[17] N. Wiberg, Lehrbuch der Anorganischen Chemie, Walter de Gruyter, Berlin, 1995.